

Enhancing Order and Porosity in a Highly Robust Tin(IV) Triphosphonate Framework

Roger K. Mah, Melanie W. Lui, and George K. H. Shimizu*

Department of Chemistry, University of Calgary, Calgary, Alberta T2N 1N4, Canada

S Supporting Information

ABSTRACT: Metal organic frameworks (MOFs) are noted for crystallinity, stability, and porosity. For many industrial challenges though, beyond stability to pore activation, porous materials require high thermal and moisture stability. Here, we report a Sn(IV) triphosphonate framework, CALF-28, that is highly robust and porous. CALF-28 was designed based on the known structure of a divalent metal phosphonate that was 2-fold interpenetrated. It has strong sustaining interactions but consequently rapidly precipitates, compromising crystallinity. Using methods to enhance order, and by analogy to the M(II) analogue, insights to the structure are ascertained and corroborated by PXRD and gas sorption analysis. CALF-28 has a surface area >500 m²/g and is stable in water.

Metal organic frameworks (MOFs) are an intriguing class of materials owing to the tunable nature of their pore sizes, shapes, and surfaces.¹ The majority of MOF materials contain carboxylate linkers, as these offer the ability to form regular clusters as secondary building units (SBUs).² These SBUs are typically sufficiently robust to sustain pores as confirmed by gas sorption. At the same time, carboxylate coordination has sufficient kinetic reversibility to enable (single) crystalline products allowing X-ray diffraction studies to precisely determine structures. An Achilles heel of some carboxylate MOFs is their instability to water or atmospheric moisture,³ though some very stable MOFs have recently emerged.⁴

It is well-known that phosphonate linkers, being potentially dianionic functional groups, should form more robust solids.⁵ A less desirable but correlated consequence of the stronger bonding is diminished crystallinity owing to the rapid precipitation from solution before kinetic ordering can occur.⁶ Another issue with phosphonate linkers is that the pyramidal geometry of the donors creates a predisposition to forming layered materials in the absence of any strong structure directing effects.⁷ While these classic “hybrid inorganic organic” solids are often crystalline, this owes more to the efficient (dense) packing of the organic interlayer than kinetic reversibility. Numerous strategies (mixed phosphonate linkers, nonlinear linkers, mixed donor chelating phosphonates, short linkers) have evolved to circumvent this tendency, leading to a range of reported porous and crystalline metal phosphonates.⁸

Here, we report a highly robust and porous metal phosphonate designed based upon the known crystal structure

of a nonporous material. Previously, we reported the crystal structure of the complex Sr₂(H₂L), **1**.⁹ The structure, shown in Figure 1, is 2-

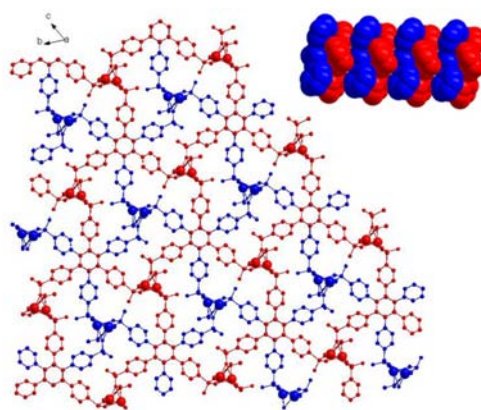


Figure 1. Sr₂(H₂L)⁹ with dual interpenetration (red + blue nets) with an inset of 60° offset grids. Inset: A space-filling view of the staggered linkers down the *a* axis.

fold interpenetrated (red and blue nets); each net consists of one-dimensional columns of phosphonate bridged Sr ions that link honeycomb assemblies of L molecules. The only contact between the interpenetrated nets is vdW in nature and is π -stacking between the central aromatic rings of the L molecules. The inset in Figure 1 shows the L molecules, with the central arene rings π -stacked, and their 60° offset orientation leading to efficient interpenetration and compromised porosity. A single net of the structure could potentially offer open pores if the structure could sustain evacuation.

On the basis of the Sr₂(H₂L) structure, **1**, the following design hypothesis was proposed to create open pores. Doubling the charge of the metal ion to a tetravalent metal would still require the same number of ligand molecules to charge compensate but only require half the number of metal ions. Thus, only half the phosphonate bridged inorganic columns would need to be present in the structure to potentially open pores. Considering the possible favorable intermolecular interactions, one would expect the L molecules to then adopt an eclipsed orientation where both electrostatic and hydrophilic interactions between the phosphonate groups and the metal ion as well as hydrophobic/ π -stacking effects between L molecules

Received: February 1, 2013

Published: June 14, 2013

would be maximized. The present study reports the pursuit of the above hypothesis through the Sn^{4+} complex of the ligand **L**, $\text{Sn}(\text{H}_2\text{L})\cdot 4.5\text{H}_2\text{O}$, CALF-28 where CALF = Calgary Framework. We report our efforts to enhance crystallinity, but ultimately CALF-28 is not able to be made single crystalline. However, it is a permanently porous solid that is stable to high levels of moisture. Moreover, the gas sorption data and accessible information from broadened powder X-ray diffraction (PXRD) data suggest the formation of the postulated structure.

The acid form of H_6L was synthesized as previously reported.⁹ The most crystalline samples of CALF-28 were prepared solvothermally using H_6L (0.075 g, 0.13 mmol), $\text{SnCl}_4\cdot 5\text{H}_2\text{O}$ (0.048 g, 0.13 mmol), and HCl (12.1 M, 0.11 mL) in MeOH (3 mL). The autoclave was heated at 120 °C over 2 h, held at 120 °C for 48 h, and cooled to room temperature over 12 h, resulting in a white powder; this powder was ground up and placed in a humidity oven at 80 °C at 90% relative humidity for 24 h, resulting in CALF-28. CALF-28 is not a highly crystalline material, and the given preparation is optimized.

Many variables (anions, pH control, crystallization methods, heating cycles) were explored to optimize the CALF-28 synthesis. Using only $\text{SnCl}_4\cdot 5\text{H}_2\text{O}$ or $\text{Sn}(\text{OAc})_4$ through reflux, hydro(solvo)thermal, or various solvent diffusions, an amorphous product (Figure S1) always formed. To increase order, acetic acid was added to shift the equilibrium from the product. Adding acetic acid in autoclaves at 120 °C gave a broad peak in the PXRD centered at 6.3° (Figure S2) indicating some ordering. Unfortunately, using $\text{Sn}(\text{OAc})_4$ gave SnO_2 as well as CALF-28, prompting the change to $\text{SnCl}_4\cdot 5\text{H}_2\text{O}$ with HCl as an auxiliary acid. This gave a similar broad peak at 6.2° (Figure S2) but without SnO_2 . To slow the complexation and enhance crystallinity, solvent diffusions and slow evaporations were (unsuccessfully) attempted using H_6L , $\text{SnCl}_4\cdot 5\text{H}_2\text{O}$, and HCl. Finally, the heating cycle's temperatures (80, 100, 120, 150, and 180 °C), hold times (48, 96 h), and cool down times (12, 48 h) were varied. Order increased from 100 to 120 °C with no change above 120 °C. Longer hold and cool times did not improve ordering. The humidity treatment is critical in reproducing CALF-28. Reactions with only water in the autoclave were unsuccessful due to insolubility of H_6L . With 1:4 $\text{H}_2\text{O}/\text{MeOH}$ mixtures, the product obtained was a mixture of amorphous CALF-28 and unreacted H_6L . Ratios above 1:1 $\text{H}_2\text{O}/\text{MeOH}$ gave unreacted H_6L . Though CALF-28 is not highly ordered, through a combination of techniques, meaningful insights to the structure are attainable.

The molecular formula of CALF-28 was determined from elemental analysis (EA) and energy dispersive X-ray spectroscopy (EDX). The EA results revealed C, 38.81% and H, 3.26% (calcd. C, 38.84%; H, 3.53% for $\text{SnH}_2\text{L}\cdot (\text{H}_2\text{O})_{4.5}$). The EDX data provided a Sn/P ratio of 1:3.2, a reasonable correlation, given the less ordered nature of the solid, to the expected Sn/P of 1:3.0 given the molecular formula determined from EA. Thermogravimetric analysis showed that CALF-28 is stable up to 450 °C (Figure S3); the initial mass loss is included solvent. The PXRD pattern (Figure S4) consists of a low angle peak at 6.1° with a small shoulder. The low angle peak correlates with a d spacing of 14.4 Å. Within a layer of **1**, the spacing between repeat units in the structure was 15.3 Å. A lower value would be expected for CALF-28; the smaller Sn radius (Sr^{2+} , 1.26 Å; Sn^{4+} , 0.81 Å) and the hypothesized removal of the interpenetration would both contribute to a contracted honeycomb

for CALF-28. The observed solvent inclusion prompted N_2 sorption to be run. For activation, CALF-28 was treated with methanol for 48 h followed by heating at 100 °C for 16 h. The 77 K N_2 isotherm (Figure 2a) is a type I isotherm as expected

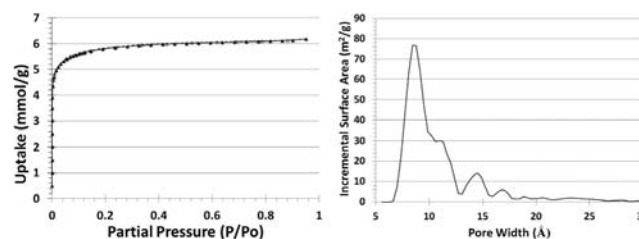


Figure 2. (a) N_2 (77 K) isotherm for CALF-28. (b) NLDFT pore size distribution from N_2 isotherm with maximum at 8.5 Å.

for a microporous solid. The BET surface area is 502 m^2/g (Langmuir: 531 m^2/g), considerably higher than the surface area of **1**⁹ (146 m^2/g from CO_2 at 273 K, nonporous to N_2 at 77 K). The increased surface area supported the removal of the interpenetration in **1** by switching from Sr^{2+} to Sn^{4+} . From the N_2 isotherm, a pore size distribution was modeled using nonlocal density functional theory, giving a peak at 8.5 Å (Figure 2b). A single net of **1** has a pore size of 10.5 Å (Figure S5) accounting for vdW radii; this would resemble the hypothesized CALF-28. An 8.5 Å pore is reasonable for CALF-28 given the structural contraction observed in the PXRD pattern. This also corroborates the removal of interpenetration in CALF-28 giving accessible pores. IR spectra (Figure S6) showed that CALF-28, like $\text{Sr}_2(\text{H}_2\text{L})$, did not possess C_3 symmetrically coordinated PO_3 groups but both coordinated (1050–950 cm^{-1}) and free P–O (1150 cm^{-1}) groups.

CALF-28 is robust and water stable. As part of the synthesis, CALF-28 is exposed to high humidity conditions (80 °C, 90% relative humidity for 24 h). Prior to the humidity treatment, products from similar preparations give variable (700–800 m^2/g) surface areas and bimodal pore distributions. After humidity treatment, the N_2 isotherms at 77 K reveal a diminished surface area (Figure S7), but this structure is reproducible and stable. Accompanying the change in surface area is a very notable shift from a bimodal pore distribution (Figure S8) prior to humidity treatment (peaks at 7.5–8 Å and 9.5–11.5 Å) to a pore distribution with a peak at 8.5 Å consistent with increased order. Further humidity treatment results in no further observable changes to porosity or pore distribution.

Given the porosity and water stability of CALF-28, CO_2 sorption was carried out. Figure 3 shows a CO_2 uptake of 2.17 mol/g (1.2 bar, 273 K) and 2.51 mol/g (1.2 bar, 263 K). The selectivity for CO_2/N_2 was determined as 14.8 based on Henry's constants of 298 K isotherms (Figure S9). The corresponding heat of adsorption (HOA), calculated using a virial model (Figure S10) is 27–25 kJ/mol, indicative of adsorption on a primarily nonpolar surface. The modest HOA aligns with the proposed structure where there are no high energy sites (bare metals or polarizing groups) directed into the pores. Retention of the porosity, after humidity conditions harsher than in a flue stream, is significant for the design of better sorbents.

MOFs are noted for their crystallinity and porosity. While itself not a crystalline material, insights into CALF-28 were obtained by analogy to the known and related network,

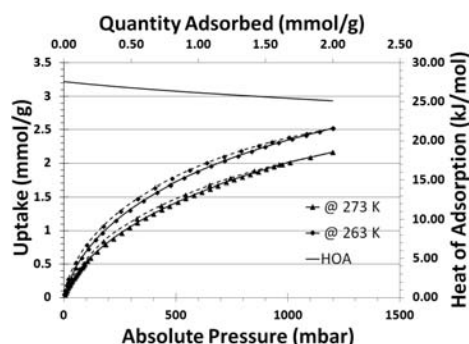


Figure 3. CO₂ isotherms at 263 K/273 K with isosteric heat of adsorption on secondary x and y axes.

Sr₂(H₂L), that formed an interpenetrated, less porous structure. With the growing emphasis on the requirement of moisture stability, for CALF-28, consideration was given to forming a robust and porous, albeit less-ordered, material rather than a less stable crystalline material. We have presented the amorphous but highly robust and porous material, CALF-28. Increasing order required optimization of numerous synthetic parameters, and characterization was through noncrystallographic means. CALF-28 shows reproducible porosity even with repeated exposure to very harsh humid conditions. The molecular formula was confirmed by EA and EDX and a structure proposed based on PXRD and N₂ gas sorption data. Although less ordered, design by ligand variation can still be applied in this case, and CALF-28 is a stepping stone for other porous materials with high water and thermal stability.

■ ASSOCIATED CONTENT

● Supporting Information

Synthesis, PXRD, gas sorption analysis, and SEM-EDX analysis for CALF-28. This material is available free of charge via the Internet at <http://pubs.acs.org>.

■ AUTHOR INFORMATION

Corresponding Author

*E-mail: gshimizu@ucalgary.ca.

Author Contributions

The manuscript was written through contributions of all authors. All authors have given approval to the final version.

Notes

The authors declare no competing financial interest.

■ ACKNOWLEDGMENTS

We thank Carbon Management Canada for financial support. M.W.L. thanks NSERC of Canada for an Undergraduate Summer Research Award.

■ REFERENCES

- (1) (a) Horcajada, P.; Gref, R.; Baati, T.; Allan, P. K.; Maurin, G.; Couvreur, P.; Férey, G.; Morris, R. E.; Serre, C. *Chem. Rev.* **2012**, *112*, 1232–1268. (b) Kreno, L. E.; Leong, K.; Farha, O. K.; Allendorf, M.; Van Duyne, R. P.; Hupp, J. T. *Chem. Rev.* **2012**, *112*, 1105–1125. (c) Li, J.-R.; Sculley, J.; Zhou, H.-C. *Chem. Rev.* **2012**, *112*, 869–932. (d) Tanabe, K. K.; Cohen, S. M. *Chem. Soc. Rev.* **2011**, *40*, 498.
- (2) (a) Perry, J. J.; Perman, J. A.; Zaworotko, M. J. *Chem. Soc. Rev.* **2009**, *38*, 1400–1417. (b) Stock, N.; Biswas, S. *Chem. Rev.* **2012**, *112*, 933–969. (c) Eddaoudi, M.; Moler, D. B.; Li, H. L.; Chen, B. L.; Reineke, T. M.; O’Keeffe, M.; Yaghi, O. M. *Acc. Chem. Res.* **2001**, *34*, 319–330.

(3) Schoenecker, P. M.; Carson, C. G.; Jasuja, H.; Flemming, C. J. J.; Walton, K. S. *Ind. Eng. Chem. Res.* **2012**, *51*, 6513–6519.

(4) (a) Cavka, J. H.; Jakobsen, S.; Olsbye, U.; Guillou, N.; Lamberti, C.; Bordiga, S.; Lillerud, K. P. *J. Am. Chem. Soc.* **2008**, *130*, 13850–13851. (b) Guillermin, V.; Ragon, F.; Dan-Hardi, M.; Devic, T.; Vishnuvarthan, M.; Campo, B.; Vimont, A.; Clet, G.; Yang, Q.; Maurin, G.; Férey, G.; Vittadini, A.; Gross, S.; Serre, C. *Angew. Chem., Int. Ed.* **2012**, *51*, 9267–9271. (c) Park, K. S.; Ni, Z.; Cote, A. P.; Choi, J. Y.; Huang, R. D.; Uribe-Romo, F. J.; Chae, H. K.; O’Keeffe, M.; Yaghi, O. M. *Proc. Natl. Acad. Sci. U. S. A.* **2006**, *103*, 10186–10191. (d) Cychoz, K. A.; Matzger, A. J. *Langmuir* **2010**, *26*, 17198–17202. (e) Chen, S. S.; Chen, M.; Takamizawa, S.; Chen, M. S.; Su, Z.; Sun, W. Y. *Chem. Commun.* **2011**, *47*, 752–754. (f) Choi, H. J.; Dinca, M.; Dailly, A.; Long, J. R. *Energy Environ. Sci.* **2010**, *3*, 117–123. (g) Demessence, A.; D’Alessandro, D. M.; Foo, M. L.; Long, J. R. *J. Am. Chem. Soc.* **2009**, *131*, 8784–8786. (h) Li, T.; Chen, D.-L.; Sullivan, J. E.; Kozlowski, M. T.; Johnson, J. K.; Rosi, N. L. *Chem. Sci.* **2013**, *4*, 1746–1755. (i) Lu, Z.; Xing, Sun, R.; Bai, J.; Zheng, B.; Li, Y. *Cryst. Growth Des.* **2012**, *12*, 1081–1084.

(5) (a) Mao, J. G. *Coord. Chem. Rev.* **2007**, *251*, 1493. (b) Clearfield, A. *Prog. Inorg. Chem.* **1998**, *47*, 371.

(6) (a) Vasylyev, M.; Neumann, R. *Chem. Mater.* **2006**, *18*, 2781–2783. (b) Dutta, A.; Pramanik, M.; Patra, A. K.; Nandi, M.; Uyama, H.; Bhaumik, A. *Chem. Commun.* **2012**, *48*, 6738–6740. (c) Khan, N. A.; Kang, I. J.; Seok, H. Y.; Jung, S. H. *Chem. Eng. J.* **2011**, *166*, 1152–1157.

(7) (a) Serre, C.; Groves, J. A.; Lightfoot, P.; Slawin, A. M. Z.; Wright, P. A.; Stock, N.; Bein, T.; Haouas, M.; Taulelle, F.; Férey, G. *Chem. Mater.* **2006**, *18*, 1451. (b) Miller, S. R.; Pearce, G. M.; Wright, P. A.; Bonino, F.; Chavan, S.; Bordiga, S.; Margiolaki, I.; Guillou, N.; Férey, G.; Borelly, S.; Llewellyn, P. L. *J. Am. Chem. Soc.* **2008**, *130*, 15967. (c) Lohse, D. L.; Sevov, S. C. *Angew. Chem., Int. Ed. Engl.* **1997**, *36*, 1619. Dines, M. B.; Cooksey, R. E.; Griffith, P. C.; Lane, R. H. *Inorg. Chem.* **1983**, *22*, 1003. (d) Maeda, K.; Kiyozumi, Y.; Mizukami, F. *Angew. Chem., Int. Ed. Engl.* **1994**, *33*, 2335. (e) Maeda, K.; Akimoto, J.; Kiyozumi, Y.; Mizukami, F. *J. Chem. Soc., Chem. Commun.* **1995**, 1033. (f) Liang, J.; Shimizu, G. K. H. *Inorg. Chem.* **2007**, *46*, 10449. (g) Taylor, J. M.; Mahmoudkhani, A. M.; Shimizu, G. K. H. *Angew. Chem., Int. Ed.* **2007**, *46*, 795.

(8) (a) Colodrero, R. M. P.; Papathanasiou, K. E.; Stavgiannoudaki, N.; Olivera-Pastor, P.; Losilla, E. R.; Aranda, M. A. G.; Leon-Reina, L.; Sanz, J.; Sobrados, I.; Choquesillo-Lazarte, D.; Garcia-Ruiz, J. M.; Atienzar, P.; Rey, F.; Demadis, K. D.; Cabeza, A. *Chem. Mater.* **2012**, *24*, 3780–379. (c) Costantino, F.; Donnadio, A.; Casciola, M. *Inorg. Chem.* **2012**, *51*, 6992–7000. (d) Lin, X. Z.; Yuang, Z. Y. *Eur. J. Inorg. Chem.* **2012**, 2661–2664. (e) Dutta, A.; Patra, A. K.; Bhaumik, A. *Microporous Mesoporous Mater.* **2012**, *155*, 208–214. (f) Dong, D. P.; Liu, L.; Sun, Z. G.; Jiao, C. Q.; Liu, Z. M.; Li, C.; Zhu, Y. Y.; Chen, K.; Wang, C. L. *Cryst. Growth Des.* **2011**, *11*, 5346–5354. (g) Adelan, P. O.; Albrecht-Schmitt, T. E. *J. Solid State Chem.* **2011**, *184*, 2368–2373. (h) Ayi, A. A.; Burrows, A. D.; Mahon, M. F.; Pop, V. M. *J. Chem. Crystallogr.* **2011**, *41*, 1165–1168. (i) Rocha, J.; Paz, F. A. A.; Shi, F. N.; Ananias, D.; Silva, N. J. O.; Carlos, L. D.; Trindade, T. *Eur. J. Inorg. Chem.* **2011**, 2035–2044. (j) Brunet, E.; Alhendawi, H. M. H.; Cerro, C.; de la Mata, M. J.; Juanes, O.; Rodriguez-Ubis, J. C. *Microporous Mesoporous Mater.* **2011**, *138*, 75–85.

(9) Vaidhyanathan, R.; Mahmoudkhani, A. H.; Shimizu, G. K. H. *Can. J. Chem.* **2009**, *87*, 247–253.